Published in final edited form as:
J Phys Chem Lett. 2010 June 1; 1(13): 1952–1956. doi:10.1021/jz100564j.

Broadband Heteronuclear Solid-State NMR Experiments by Exponentially Modulated Dipolar Recoupling without Decoupling

Anders B. Nielsen[¶], **Lasse A. Straasø**[¶], **Andrew J. Nieuwkoop**[§], **Chad M. Rienstra**[§], **Morten Bjerring**[¶], and **Niels Chr. Nielsen**[¶,*]

[¶]Center for Insoluble Protein Structures (inSPIN), Interdiscipolinary Nanoscience Center (iNANO) and Department of Chemistry, Aarhus University, DK-8000 Aarhus C, Denmark.

[§]Department of Chemistry, University of Illinois, A120 Chemical & Life Sciences Lab 600 South Mathews Avenue Urbana, USA.

Abstract

We present a novel solid-state NMR method for heteronuclear dipolar recoupling without decoupling. The method, which introduces the concept of exponentially modulated rf fields, provides efficient broadband recoupling with large flexibility with respect to hetero- or homonuclear applications, sample spinning frequency, and operation without the need for high-power ^{1}H decoupling. For previous methods, the latter has been a severe source of sample heating which may cause detoriation of costly samples. The so-called EXPonentially mOdulated Recoupling Technique (EXPORT) is described analytically and numerically, and demonstrated experimentally by 1D ^{13}C spectra and 2D ^{13}C-^{15}N correlation spectra of ^{13}C,^{15}N-labeled samples of GB1, ubiquitin, and fibrils of the SNNFGAILSS fragment of amylin. Through its flexible operation, robustness, and strong performance, it is anticipated that EXPORT will find immediate application for both hetero- and homonuclear dipolar recoupling in solid-state NMR of ^{13}C,^{15}N-labeled proteins and compounds of relevance in chemistry.

Keywords

Solid-State NMR; Dipolar recoupling without decoupling; proteins

Over the past few years solid-state NMR has demonstrated capability to undertake a long-standing need in structural biology, namely resolving atomic-resolution structure and dynamics information for so-called insoluble proteins that reside in, e.g., membranes,[1–7] filaments,[8] and amyloid fibrils.9–14 This has been facilitated by development of advanced instrumentation, isotope-labeling procedures,15–17 and pulse sequences extracting information from isotropic and anisotropic nuclear spin interactions to provide information about molecular structure and dynamics. Particular efforts have been devoted to the design of experiments which combines the high-resolution properties of magic-angle spinning (MAS) and recoupling methods to probe desired nuclear spin interactions while not using excessively long periods of strong rf irradiation.

To reduce sample detoriating effect of high-frequency rf heating focus has recently been devoted to the design of experiments that enable recoupling of dipolar interactions between low-γ nuclei without the need for intense ^{1}H irradiation for decoupling of dipolar interactions to protons. Until now this has been realized for experiments recoupling

ncn@inano.dk.

homonuclear ^{13}C-^{13}C couplings, as introduced through the experiments CMAR,[18] RFDR without decoupling,[19,20] and variants of these.[21] For the important class of heteronuclear recoupling experiments, being fundamental in solid-state NMR relying on ^{13}C,^{15}N-labeled compounds, broadband recoupling under fast MAS and high-field conditions in combination with released demands to decoupling remains a challenge.

In this Letter, we introduce a novel concept for dipolar recoupling taking advantage of multi-axis phase-modulated rf irradiation to enable recoupling of heteronuclear dipolar couplings with (*a*) extreme broadbandedness even at high field, (*b*) high efficiency through γ-encoded recoupling,[22] (*c*) compensation for rf inhomogeneity, (*d*) operation at all relevant spinning frequencies, and (*e*) realization without high-power ^1H decoupling. This is accomplished by introducing exponentially modulated rf fields which, with inspiration from recent multiple-field-oscillating recoupling methods,[23,24] exploit the effect of two intertwined modulations to facilitate simultaneous ^{13}C-^{15}N (or ^{13}C-^{13}C) recoupling and ^1H decoupling. The method will be referred to as the EXPonentially mOdulated Recoupling Technique (EXPORT).

The recoupling experiment, illustrated schematically in Fig. 1, is governed by the rf Hamiltonian

$$H_{rf}=C_I I_x+C_S S_x+B_I e^{iC_I tI_x} I_y e^{iC_I tI_x}+B_S e^{iC_S tS_x} S_y e^{iC_S tS_x} \quad (1)$$

where I_q and S_q (q=x,y,z) represent Cartesian operators for the I and S spins, respectively, and B_I, B_S, C_I, and C_S amplitudes for the I- and S-spin components of the rf field. Although the method works equally well for homonuclear dipolar recoupling, we here restrict ourselves to the heteronuclear case with I=^{15}N and S=^{13}C. In pratice, the rf fields may be expessed in terms of an amplitude $A_K(t)=\sqrt{C_K^2+(B_K\cos(C_K t))^2}$ and phase $\phi_K(t)=\tan^{-1}\left(\frac{B_K\cos(C_K t)}{C_K}\right)+\frac{B_K}{C_K}(\cos(C_K t)-1)$ (K=I or S). While the use of different C_K values on the two rf channels offers interesting possibilities to adapt the rf fields most appropriately to the instrumentation and specific desires in terms of broadbandedness, we will for the sake of simplicity assume C=C_I=C_S.

The impact of the rf field on chemical shift and dipolar couplings may be described by transforming the Hamiltonians for these interactions, $H_K(t)=\omega_K(t)K_z$ and $H_{IS}(t)=\omega_{IS}(t)2I_z S_z$, respectively, into the interaction frame of the rf irradiation. By first transforming into the frame of the modulating field $C(I_x+S_x)$ using $\tilde{F}(t)=e^{iCt(I_x+S_x)}Fe^{-iCt(I_x+S_x)}$ and subsequently into the frame of the weak rf fields $B_I I_y$ and $B_S S_y$ using $\tilde{\tilde{F}}(t)=e^{iB_I tI_x}e^{iB_S tS_x}\tilde{F}(t)e^{-iB_S tS_x}e^{-iB_I tI_x}$ one arrives at

$$\tilde{\tilde{H}}_K(t)=\omega_K(t)\left[-c_{Ct}s_{B_K t}I_x+s_{Ct}I_y+c_{Ct}c_{B_K t}I_z\right] \quad (2)$$

$$\tilde{\tilde{H}}_{IS}(t)=2\omega_{IS}(t)[\, s_{C_t}^2 I_y S_y + c_{C_t}^2 \left(c_{B_{I^t}} c_{B_{S^t}} I_z S_z + s_{B_{I^t}} s_{B_{S^t}} I_x S_x - c_{B_{I^t}} s_{B_{S^t}} I_z S_x - s_{B_{I^t}} c_{B_{S^t}} I_x S_z\right) + s_{C_t} c_{C_t} \left(c_{B_{I^t}} I_z S_y + c_{B_{S^t}} I_y S_z - s_{B_{I^t}} I_y S_x - s_{B_{S^t}} I_x S_y\right)] \quad (3)$$

using the shorthand notation c_x=cos(x) and s_x=sin(x). By assuming C>>B_I,B_S,ω_r, it is evident that all linear terms (eq. (2)) – covering chemical shift on the I and S spins as well as dipolar couplings to protons (the Hamiltonian is modified by multiplying with $2H_z$, with H_z being the ^{1}H Zeeman operator, and changing the angular frequency to that of the coupling) vanish to first-order upon averaging over the period 1/C. It can also be shown that the first and third of the three terms within the square bracket in eq. (3) does not lead to recoupling.

Using $\omega_{IS}(t)=\sum_{m=-2}^{2} \omega_{IS}^{(m)} e^{im\omega_r t}$ with the Fourier coefficients given elsewhere,[25] the second term lead to the first-order average over the period 1/|B_I−B_S|:

$$\overline{\tilde{\tilde{H}}}_{IS}(B_I \pm B_S = n\omega_r)=\kappa_n[\, c_{n\gamma_{PR}} (I_z S_z \mathrm{m} I_x S_x) - s_{n\gamma_{PR}} (I_x S_z \mathrm{m} I_z S_x)] \quad (5)$$

using $\kappa_{\pm 1}=b_{IS} s_{2\beta_{PR}}/(4\sqrt{2})$ and $\kappa_{\pm 2}=-b_{IS} s_{\beta_{PR}}^2/8$ with $b_{IS}=-\gamma_I\gamma_S\mu_o/(4\pi r_{IS}^3)$ denoting the dipole-dipole coupling in angular units and β_{PR} and γ_{PR} the polar an azimutal angles, respectively, relating the internuclear axis to the rotor axis. It is evident that γ_{PR}-encoded[22] zero- or double-quantum dipolar recoupling (in a frame tilted by $\pi/2$ around I_y and S_y) may be obtained by adjusting the sum and difference of the recoupling B_I and B_S field amplitudes to match $n\omega_r$ (n=±1 or ±2). Efficient cancellation of chemical shift and couplings to protons and avoiding interference with recoupling require that the decoupling field C is substantially larger than the B fields. Effects from rf inhomogeneity may be reduced by phase-alternating ±C for each $\tau_C=\tau_r/C$ as illustrated by the E and $\bar{E}$ elements in Fig. 1.

Independent adjustment of the recoupling and decoupling fields opens up the possibility to perform experiments with (small values of C) or without (large values of C) ^{1}H decoupling with great flexibility on the spinning frequency. This solves a major problem for heteronuclear dipolar recoupling, where typical combinations of recoupling fields at the low-γ spins species and simultaneous need for high-power ^{1}H decoupling (typical recommendation: $\omega_{rf}(^1\mathrm{H}) > 2.5\omega_{rf}(I,S)$) may lead to excessively strong ^{1}H rf fields in the regime of medium to fast sample spinning with the inherent risk of sample damage. We note that at very spinning frequencies (>35 kHz), ^{1}H decoupling with low rf field strengths may be feasible.[26,27]

Through numerical simulations of ^{15}N to $^{13}C_\alpha$ coherence transfer in a typical ^{15}N-$^{13}C_\alpha$ spin-pair system at 16.4 T using MAS with $\omega_r/2\pi$=12 kHz, Fig. 2c demonstrates that EXPORT (C=6ω_r, B_I=3ω_r/8, and B_S=5ω_r/8) is substantially more robust with respect to resonance offsets than standard double-cross-polarization[29] (DCP, $\omega_{rf,N}$=3ω_r, $\omega_{rf,C}$=4ω_r) (Fig. 2a) and the deliberately bandselective ^{OC}NCA experiment (Fig. 2b).[28] EXPORT is also superior to previous experiments with respect to rf mismatch (and thereby rf inhomogenity) as illustrated in Figs. 2d–2f by numerical simulations for DCP (Fig. 2d), EXPORT with the rf wave digitized in 100 (Fig. 2e) and 20 (Fig. 2f) steps over each rotor period. Figures 2e and

2f also illustrate an important issue of EXPORT, namely the need for good digitization of the *C*-field phase modulation. Too low digitization may degrade the sensitivity of the experiment, but conversely improve the robustness towards rf inhomogeneity.

Experimental data in Fig. 3, obtained at 16.4 T for a fibrillar sample of the hIAPP20-29 decapeptide (SNNFGAILSS) of amylin with uniform $^{13}C,^{15}N$ labeling of the FGAIL stretch using a 1D version of the pulse sequence in Fig. 1 with 11.9 kHz spinning, clearly reinforces that EXPORT in addition to the clear advantage of recoupling without decoupling facilitates experimental realization through robustness towards rf mismatch and inhomogeneity. We note that the doubled number of peaks is a result of antiparallel fibril formation.[13] Figure 3 illustrates experimentally and numerically the consequences of rf mismatch on the ^{13}C rf channel for ^{15}N to $^{13}C_\alpha$ (NCA, Fig. 3a) and ^{15}N to $^{13}C'$ (NCO, Fig. 3b) coherence transfers for EXPORT (open circles; $C=7\omega_r$, $B_I=3\omega_r/8$, $B_S=5\omega_r/8$, no decoupling) and a carefully optimized DCP sequence (crosses; $\omega_{rf,C}/(2\pi)$ = 50.2 kHz, $\omega_{rf,N}/(2\pi)$ = 39.3 kHz with 120 kHz CW ^1H decoupling). Both experiments and simulations took into account 5% Lorentzian rf inhomogeneity, which along with a relatively course digitization (time steps of 1.2 μs) reduces the overall transfer to 0.4–0.5 in this specific case. We note that the corresponding homonuclear experiments are considerably less influenced by digitization and rf inhomogeneity effects. Nonetheless, the experiments (including the representative spectra in Figs. 3c and 3d) and the good numerical reproductions clearly highlight the robustness of EXPORT relative to DCP with respect to rf field variations, which removes one of the major drawbacks of DCP, namely the need for very precise calibrations and long-term stability of the involved rf field strengths. It should be mentioned that under the present modest sample-spinning conditions some intensity loss is observed for the methylene groups using EXPORT without decoupling, which is understandable considering the strong couplings present in this system and the associated general difficulties in decoupling of methylene carbons.

Figure 4a illustrates the use of EXPORT to obtain ^{15}N-^{13}C 2D chemical shift correlation for a uniformly-$^{13}C,^{15}N$-labelled sample of the β_1-domain of the immunoglobulin binding protein G (GB1)[33] at 23.81 kHz spinning without ^1H decoupling during the ^{13}C-^{15}N mixing. The static fields were adjusted to $C=3\omega_r$ (i.e., 71.5 kHz) with the ^{13}C rf carrier between the $^{13}C_\alpha$ and $^{13}C'$ regions leading to efficient transfer to both types of spins. We note that recoupling without decoupling may alternatively be obtained using DCP or adiabatic variants with comparatively strong rf fields on the ^{13}C and ^{15}N channels, although with higher sensitivity towards rf inhomogeneity and mismatch. In Fig. 4b, we experimentally demonstrate the broadband recoupling of $^{13}C,^{15}N$ dipolar interactions for EXPORT on *U*-$^{13}C,^{15}N$-ubiquitin at 10.02 kHz spinning, using $C=3\omega_r$, $B_I=3\omega_r/8$, and $B_S=5\omega_r/8$. By varying the ^{13}C carrier frequency, polarization can be directed to both $^{13}C_\alpha$'s and $^{13}C`$'s (top) or in a band-selective manner to either $^{13}C_\alpha$'s (middle) or $^{13}C`$'s (bottom). The spectra were obtained using relatively weak $^{13}C,^{15}N$ rf fields (~31 kHz) and standard ^1H CW decoupling (90 kHz) during the heteronuclear transfer.

In conclusion, we have introduced the concept of exponentially modulated dipolar recoupling and demonstrated its strong capabilities to accomplish ^{13}C-^{15}N dipolar recoupling at varying MAS frequencies with or without ^1H decoupling. Through its superior performance relative to previous methods, and the straightforward use of the EXPORT principle in numerous other applications, we anticipate that the presented methods will find widespread applications for solid-state NMR spectroscopy of biological molecules, as well as problems in materials chemistry where heteronuclear correlation experiments have broad applicability.

Acknowledgments

We acknowledge support from the Danish National Research Foundation, the Danish Natural Science Research Council, and the Danish Center for Scientific Computing. CMR acknowledges support from the National Institutes of Healt (grant no. NIH R01-GM073770).

REFERENCES

1. Etzkorn M, Martell S, Andronesi OC, Seidel K, Engelhard M, Baldus M. Secondary Structure, Dynamics, and Topology of a Seven-Helix Receptor in Native Membranes, Studied by Solid-State NMR Spectroscopy. Angew. Chem. Int. Ed 2007;46:459–462.
2. Li Y, Berthold DA, Gennis RB, Rienstra CM. Chemical shift assignment of the transmembrane helices of DsbB, a 20-kDa integral membrane enzyme, by 3D magic-angle spinning NMR spectroscopy. Protein Science 2008;17:199–204. [PubMed: 18227427]
3. Hiller M, Higman VA, Jehle S, van Rossum BJ, Kuhlbrandt W, Oschkinat H. [2,3-C-13]-labeling of aromatic residues-getting a head start in the magic-angle-spinning NMR assignment of membrane proteins. J. Am. Chem. Soc 2008;130:408–409. [PubMed: 18092784]
4. Vosegaard T, Kamihira-Ishijima M, Watts A, Nielsen NC. Helix conformations in 7TM membrane proteins determined using oriented-sample solid-state NMR with multiple residue-specific N-15 labeling. Biophys. J 2008;94:241–250. [PubMed: 17827220]
5. Yi MG, Cross TA, Zhou HX. Conformational heterogeneity of the M2 proton channel and a structural model for channel activation. Proc. Natl. Acad. Sci 2009;106:13311–13316. [PubMed: 19633188]
6. Traaseth NJ, Shi L, Verardi R, Mullen DG, Barany G, Veglia G. Structure and topology of monomeric phospholamban in lipid membranes determined by a hybrid solution and solid-state NMR approach. Proc. Natl. Acad. Sci 2009;106:10165–10170. [PubMed: 19509339]
7. Cady SD, Schmidt-Rohr K, Wang J, Soto CS, DeGrado WF, Hong M. Structure of the amantadine binding site of influenza M2 proton channels in lipid bilayers. Nature 2010;463:689–692. [PubMed: 20130653]
8. Lorieau JL, Day LA, McDermott AE. Conformational dynamics of an intact virus: Order parameters for the coat protein of Pf1 bacteriophage. Proc. Natl. Acad. Sci 2008;105:10366–10371. [PubMed: 18653759]
9. Petkova AT, Ishii Y, Balbach JJ, Antzutkin ON, Leapman RD, Delaglio F, Tycko R. A structural model for Alzheimer's beta -amyloid fibrils based on experimental constraints from solid state NMR. Proc. Natl. Acad. Sci 2002;99:16742–16747. [PubMed: 12481027]
10. van der Wel PCA, Lewandowski JR, Griffin RG. Solid-state NMR study of amyloid nanocrystals and fibrils formed by the peptide GNNQQNY from yeast prion protein Sup35p. J. Am. Chem. Soc 2007;129:5117–5130. [PubMed: 17397156]
11. Iwata K, Fujiwara T, Matsuki Y, Akutsu H, Takahashi S, Naiki H, Goto Y. 3D structure of amyloid protofilaments of beta(2)-microglobulin fragment probed by solid-state NMR. Proc. Natl. Acad. Sci 2006;103:18119–18124. [PubMed: 17108084]
12. Wasmer C, Lange A, Van Melckebeke H, Siemer AB, Riek R, Meier BH. Amyloid fibrils of the HET-s(218–289) prion form a beta solenoid with a triangular hydrophobic core. Science 2008;319:1523–1526. [PubMed: 18339938]
13. Nielsen JT, Bjerring M, Jeppesen MD, Pedersen RO, Pedersen JM, Hein KL, Vosegaard T, Skrydstrup T, Otzen DE, Nielsen NC. Unique Identification of Supramolecular Structures in Amyloid Fibrils by Solid-State NMR Spectroscopy. Angew. Chem. Int. Ed 2009;48:2118–2121.
14. Walsh P, Simonetti K, Sharpe S. Core Structure of Amyloid Fibrils Formed by Residues 106–126 of the Human Prion Protein. Structure 2009;17:417–426. [PubMed: 19278656]
15. LeMaster DM, Kushlan DM. Dynamical mapping of E-coli thioredoxin via C-13 NMR relaxation analysis. J. Am. Chem. Soc 1996;118:9255–9264.
16. Hong M, Jakes K. Selective and extensive C-13 labeling of a membrane protein for solid-state NMR investigations. J. Biomol. NMR 1999;14:71–74. [PubMed: 10382307]

17. Castellani F, van Rossum B, Diehl A, Schubert M, Rehbein K, Oschkinat H. Structure of a protein determined by solid-state magic-angle-spinning NMR spectroscopy. Nature 2002;420:98–102. [PubMed: 12422222]
18. De Paepe G, Bayro MJ, Lewandowski J, Griffin RG. Broadband homonuclear correlation spectroscopy at high magnetic fields and MAS frequencies. J. Am. Chem. Soc 2006;128:1776–1777. [PubMed: 16464061]
19. Ishii Y. C-13-C-13 dipolar recoupling under very fast magic angle spinning in solid-state nuclear magnetic resonance: Applications to distance measurements, spectral assignments, and high-throughput secondary-structure determination. J. Chem. Phys 2001;114:8473–8483.
20. Bayro MJ, Ramachandran R, Caporini MA, Eddy MT, Griffin RG. Radio frequency-driven recoupling at high magic-angle spinning frequencies: Homonuclear recoupling sans heteronuclear decoupling. J. Chem. Phys 2008;128:052321. [PubMed: 18266438]
21. Lin J, Bayro MJ, Griffin RG, Khaneja N. Dipolar recoupling in solid state NMR by phase alternating pulse sequences. J. Magn. Reson 2009;197:145–152. [PubMed: 19157931]
22. Nielsen NC, Bildsoe H, Jakobsen HJ, Levitt MH. Double-Quantum Homonuclear Rotary Resonance - Efficient Dipolar Recovery in Magic-Angle-Spinning Nuclear-Magnetic-Resonance. J. Chem. Phys 1994;101:1805–1812.
23. Khaneja N, Nielsen NC. Triple oscillating field technique for accurate distance measurements by solid-state NMR. J. Chem. Phys 2008;128:015103. [PubMed: 18190225]
24. Straaso LA, Bjerring M, Khaneja N, Nielsen NC. Multiple-oscillating-field techniques for accurate distance measurements by solid-state NMR. J. Chem. Phys 2009;130:225103. [PubMed: 19530792]
25. Bak M, Rasmussen JT, Nielsen NC. SIMPSON: A general simulation program for solid-state NMR spectroscopy. J. Magn. Reson 2000;147:296–330. [PubMed: 11097821]
26. Wickramasinghe NP, Parthasarathy S, Jones CR, Bhardwaj C, Long F, Kotecha M, Mehboob S, Fung LWM, Past J, Samoson A, Ishii Y. Nanomole-scale protein solid-state NMR by breaking intrinsic H-1 T-1 boundaries. Nature Methods 2009;6:215–218. [PubMed: 19198596]
27. Scholz I, Hodgkinson P, Meier BH, Ernst M. Understanding two-pulse phase-modulated decoupling in solid-state NMR. J. Chem. Phys 2009;130:114510. [PubMed: 19317548]
28. Kehlet C, Bjerring M, Sivertsen AC, Kristensen T, Enghild JJ, Glaser SJ, Khaneja N, Nielsen NC. Optimal control based NCO and NCA experiments for spectral assignment in biological solid-state NMR spectroscopy. J. Magn. Reson 2007;188:216–230. [PubMed: 17681479]
29. Schaefer J, Mckay RA, Stejskal EO. Double-Cross-Polarization Nmr of Solids. J. Magn. Reson 1979;34:443–447.
30. Bak M, Schultz R, Vosegaard T, Nielsen NC. Specification and visualization of anisotropic interaction tensors in polypeptides and numerical simulations in biological solid-state NMR. J. Magn. Reson 2002;154:28–45. [PubMed: 11820824]
31. Bak M, Nielsen NC. REPULSION, a novel approach to efficient powder averaging in solid-state NMR. J. Magn. Reson 1997;125:132–139. [PubMed: 9245368]
32. Fung BM, Khitrin AK, Ermolaev K. An Improved Broadband Decoupling Sequence for Liquid Crystals and Solids. J. Magn. Reson 2000;142:97–101. [PubMed: 10617439]
33. Franks WT, Zhou DH, Wylie BJ, Money BG, Graesser DT, Frericks HL, Sahota G, Rienstra CM. Magic-angle spinning solid-state NMR spectroscopy of the beta1 immunoglobulin binding domain of protein G (GB1): 15N and 13C chemical shift assignments and conformational analysis. J. Am. Chem. Soc 2005;127:12291–12305. [PubMed: 16131207]

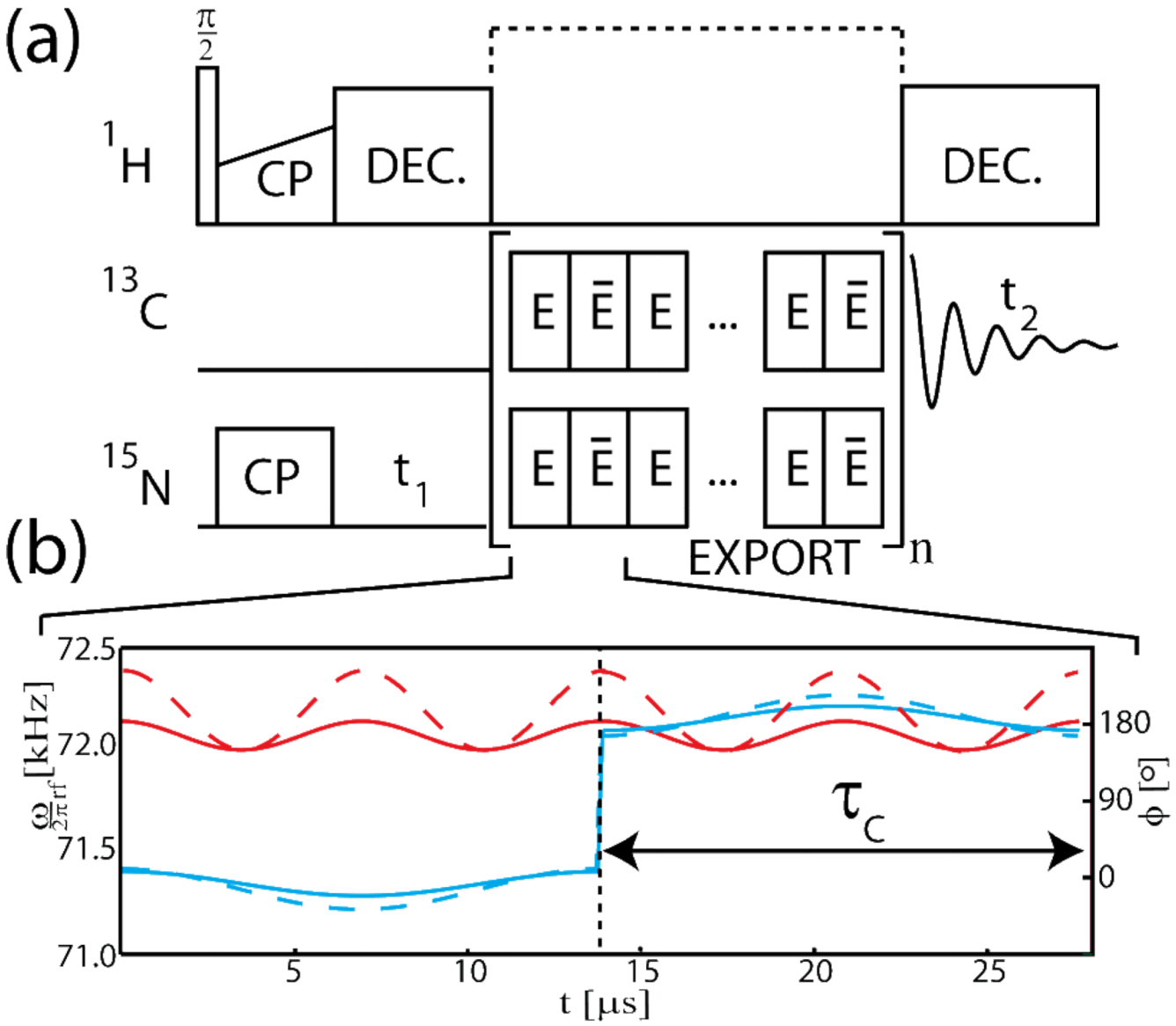

Figure 1.

(a) The EXPORT pulse sequence for heteronuclear dipolar recoupling without decoupling embedded in a typical 2D NCO/NCA chemical shift correlation experiment. (b) The amplitude (red) and phase (blue) modulation schemes of the basic elements with the ^{13}C and ^{15}N fields represented by solid and broken lines, respectively, for EXPORT with $C=6\omega_r$, $B_I=3\omega_r/8$, $B_S=5\omega_r/8$, and $\omega_r/2\pi=12$ kHz.

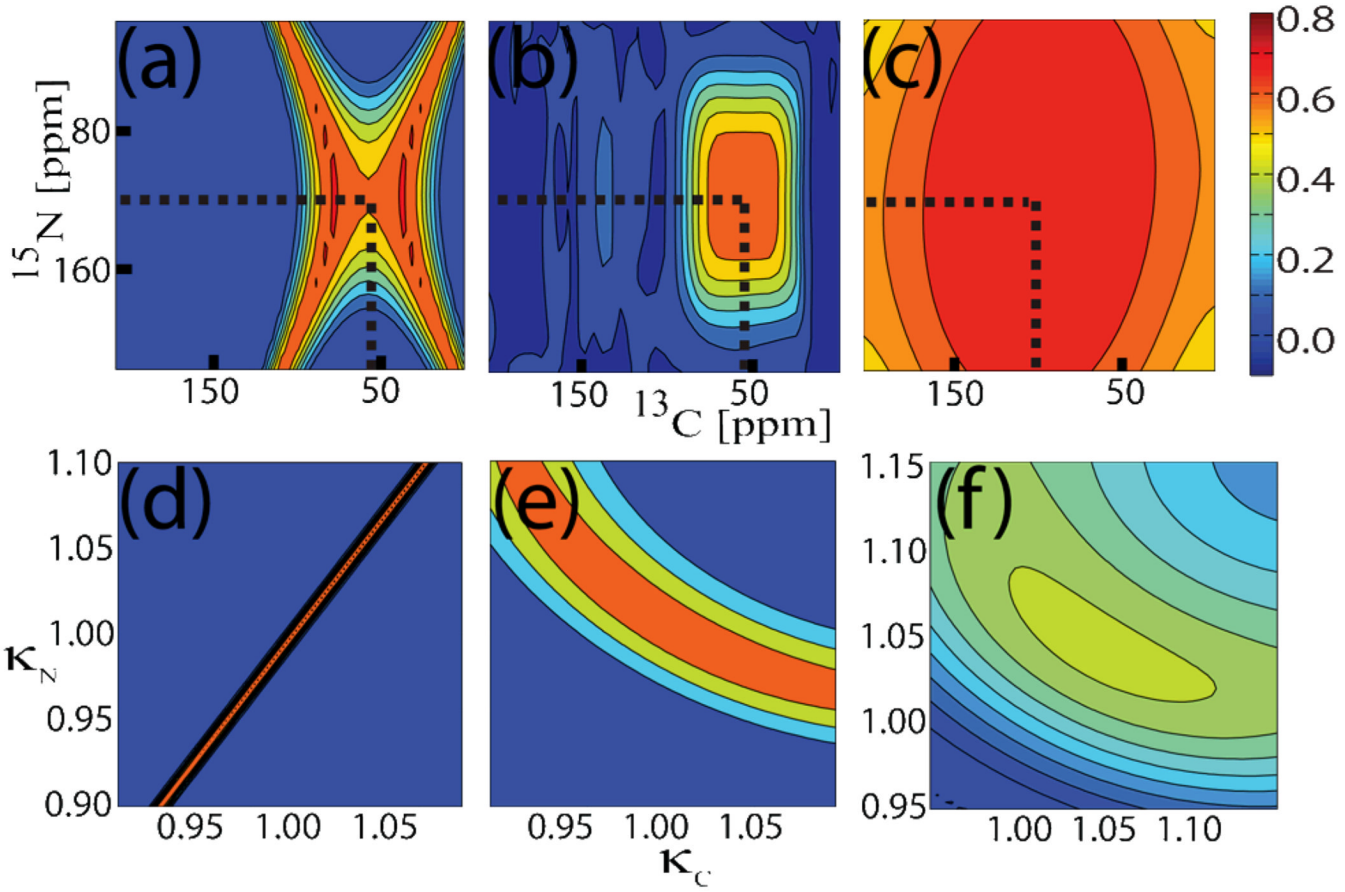

Figure 2.

^{15}N to $^{13}C_{\alpha}$ coherence transfer efficiencies calculated for EXPORT using the parameters in Fig. 1b. (a–c) 2D ^{15}N vs ^{13}C offset plots for EXPORT (c), an ^{OC}NCA optimal control sequence28 (b), and DCP (a)[29]. (d–f) 2D ^{15}N vs ^{13}C rf field strength plots (scaling factors relative to the nominal values) for DCP (d), EXPORT with high digitization of the rf field (100 points over 1 rotor period) (e), and EXPORT with lower digitization (20 points over 1 rotor period) (f). Simulations were made using SIMPSON[25] with parameters30 for a directly bonded ^{15}N-$^{13}C_{\alpha}$ spin system, powder averaging with 5 γ_{CR} and 144 REPULSION angles,[31] and a spinning frequency of 12 kHz at 16.4 T. Broken lines mark carrier frequencies.

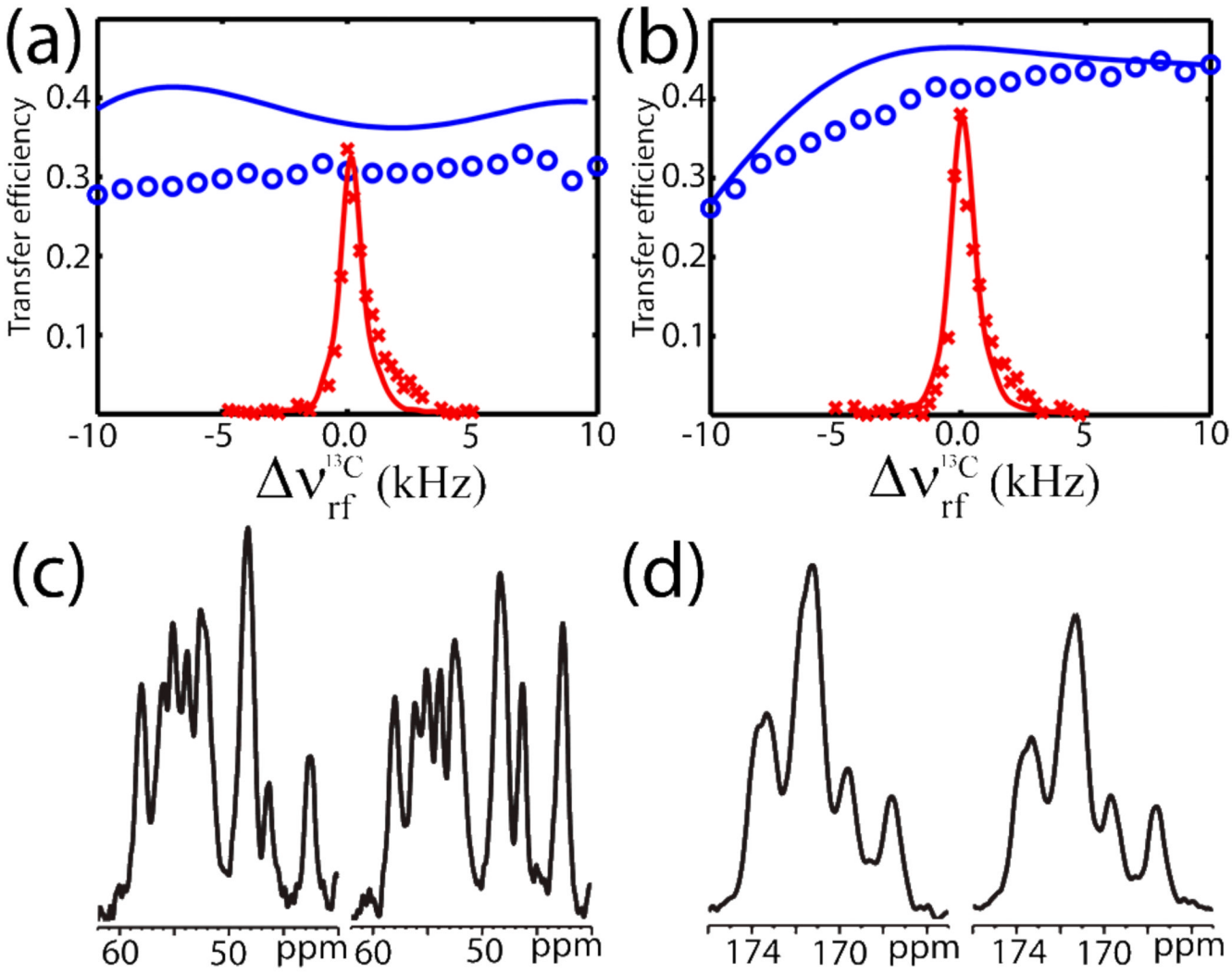

Figure 3.

Experimental (signal integrals for the target spin spectral region) and simulated ^{15}N to ^{13}C' (a) and ^{15}N to $^{13}C_{\alpha}$ (b) coherence transfer efficiencies for DCP (experiment: red crosses, simulation: red line) and EXPORT (experiment: blue circles, simulation: blue line) as function of the ^{13}C rf field strength mismatch. Experimental spectra were obtained for *U*-^{13}C,^{15}N-labeled FGAIL in a SNNFGAILSS fibril sample. Representative ^{13}C spectra following (c) ^{15}N to $^{13}C_{\alpha}$ and (d) ^{15}N to ^{13}C' transfer for EXPORT (left) and DCP (right). In accord with Fig. 1a, the spectra were recorded using CP for the initial ^{1}H-^{15}N transfer and SPINAL-64 decoupling[32] (80 kHz) was used during acqusition. All spectra were recorded at 11.9 kHz spinning with carrier frequencies at 120 ppm for ^{15}N and 50/172 ppm for NCA/NCO transfer. DCP used $\omega_{rf,C}/2\pi$ = 50.2 kHz, $\omega_{rf,N}/2\pi$ = 39.3 kHz, and 120 kHz ^{1}H decoupling. EXPORT used $C=7\omega_r$, $B_I=3\omega_r/8$, $B_S=5\omega_r/8$, and no ^{1}H decoupling.

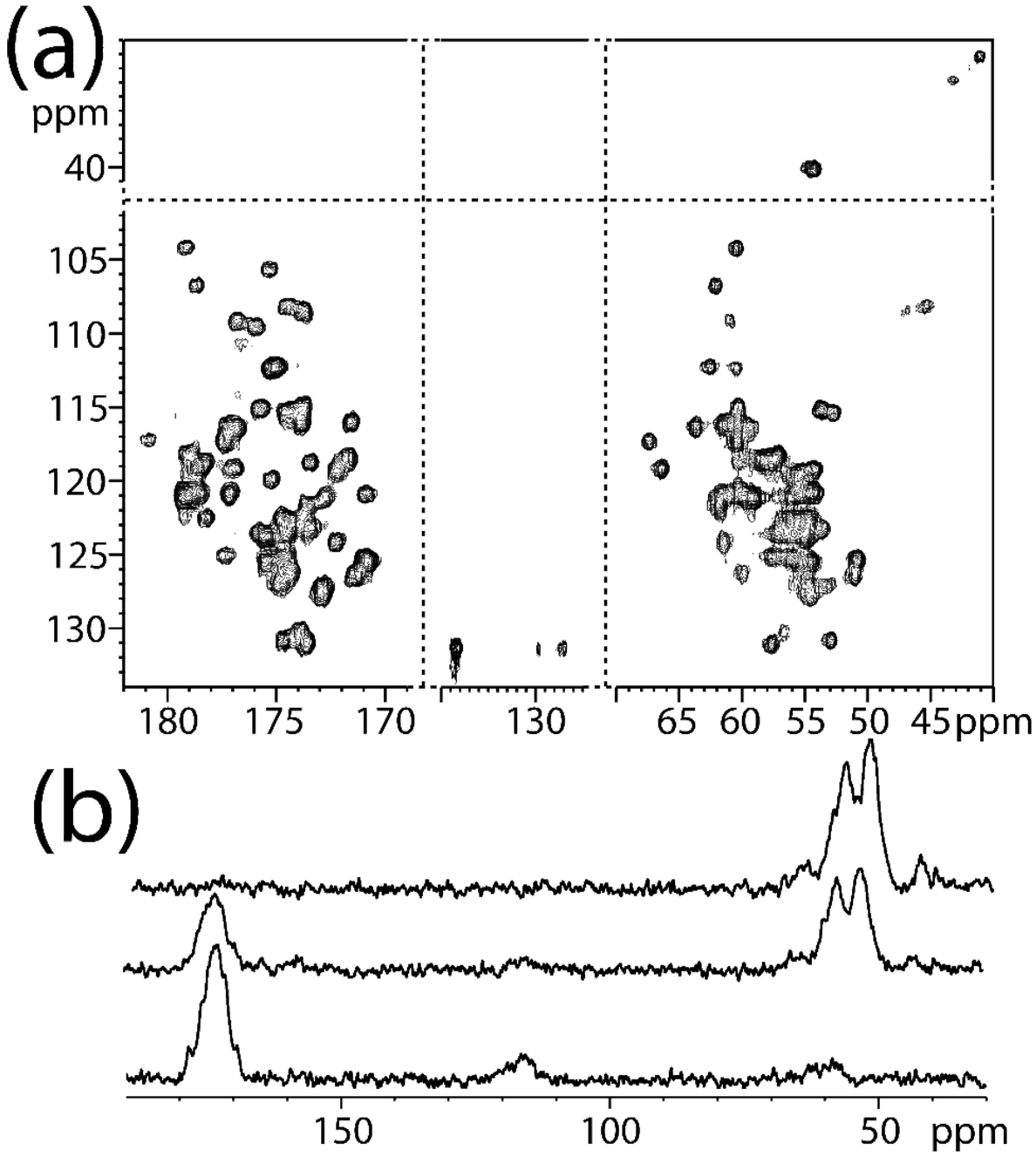

Figure 4.

Experimental spectra for *U*-^{13}C,^{15}N-labeled samples of (a) GB1 and (b) ubiquitin recorded at 16.4 T using EXPORT for ^{15}N-^{13}C transfer with $C = 3\omega_r$, $B_I = 3\omega_r/8$, $B_S = 5\omega_r/8$, and $\tau_{mix} = 2.35$ ms. In accord with Fig. 1a, the spectra were recorded using CP for the initial ^{1}H-^{15}N transfer. SPINAL-64 decoupling (70 kHz) was used in the detection periods. The 2D spectrum (a) used 23.81 kHz sample spinning without ^{1}H decoupling during EXPORT, 560 points in the indirect and 4096 point in the direct dimensions. The 1D spectra (b) used 10.02 kHz spinning, carrier frequencies at 40 (top), 120 (middle), and 180 (bottom) ppm, and 90 kHz ^{1}H decoupling during EXPORT.